A Densely Packed Sb_2O_3 Nanosheets-Graphene Aerogel toward Advanced Sodium-Ion Batteries

Jing Zhou[a], Bingyi Yan[a], Jie Yang[b], Yun Yang[b], Wei Zhou[b], Hao Lan[b], Hua Wang[b] and Lin Guo[b]**

[a.] *School of Chemistry Engineering, Northeast Electric Power University, Jilin 132012 P.R. China*

[b.] *School of Chemistry Beijing Advanced Innovation Center for Biomedical Engineering Key Laboratory of Bio-Inspired Smart Interfacial Science and Technology of Ministry of Education Beihang University, Beijing 100191, P.R. China*

E-mail: wanghua8651@buaa.edu.cn, guolin@buaa.edu.cn

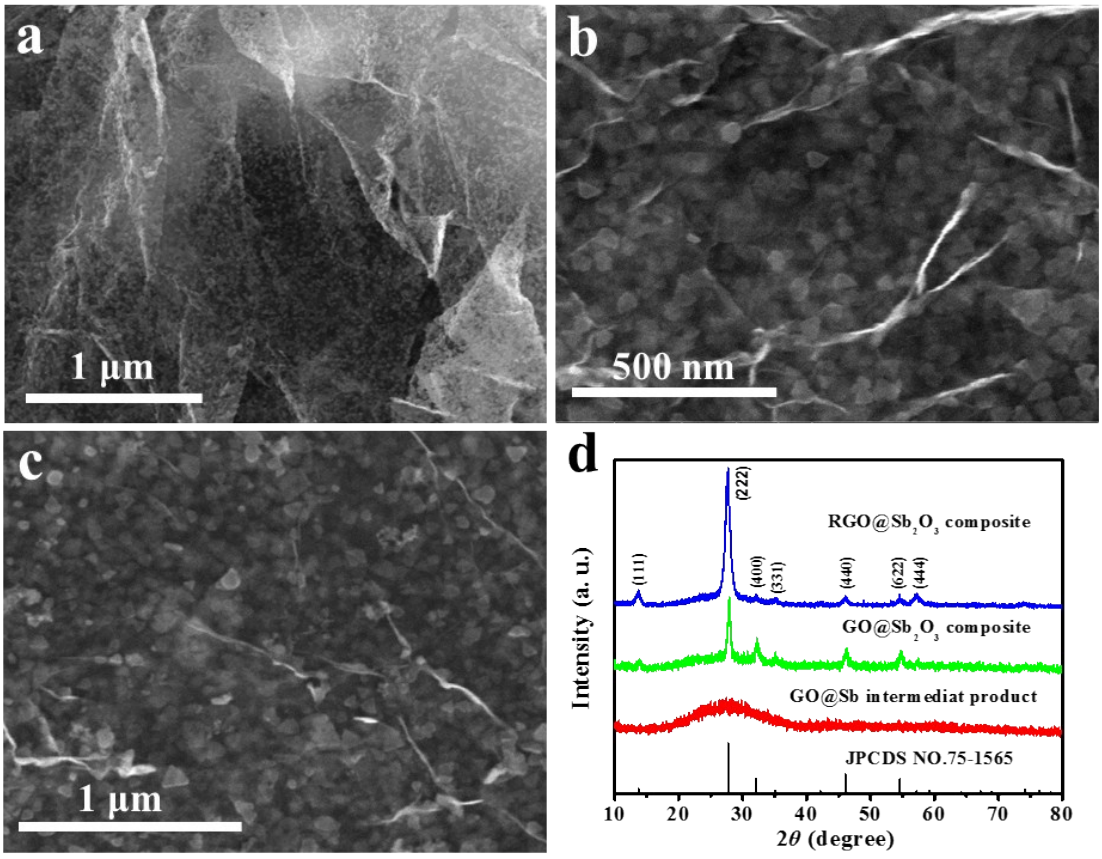

Fig S1. SEM images of (a) hydrolytic intermediate product, (b) GO@Sb_2O_3 and (c) RGO@Sb_2O_3 composites. (d) The XRD patterns of hydrolytic intermediate product, GO@Sb_2O_3 and RGO@Sb_2O_3 composites.

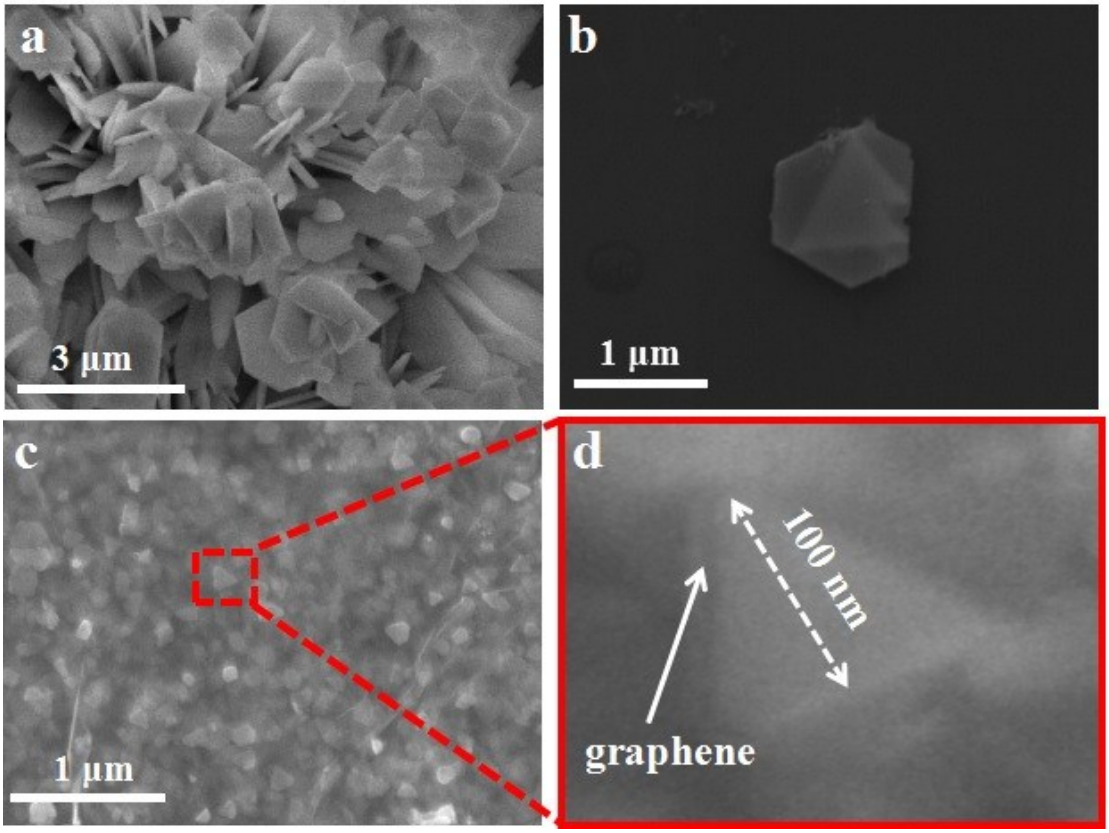

Fig S2. SEM images of (a), (b) bare Sb_2O_3 and (c), (d) RGO@Sb_2O_3.

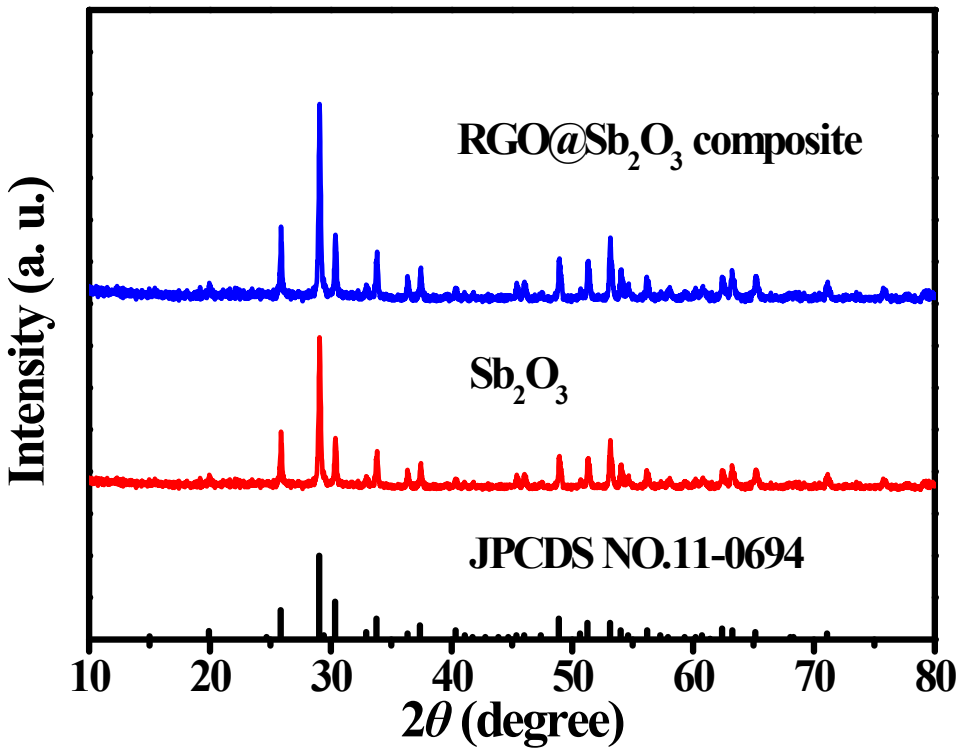

Fig S3. XRD patterns of samples obtained by annealing RGO@Sb_2O_3 and Sb_2O_3 at 800 °C in air atmosphere.

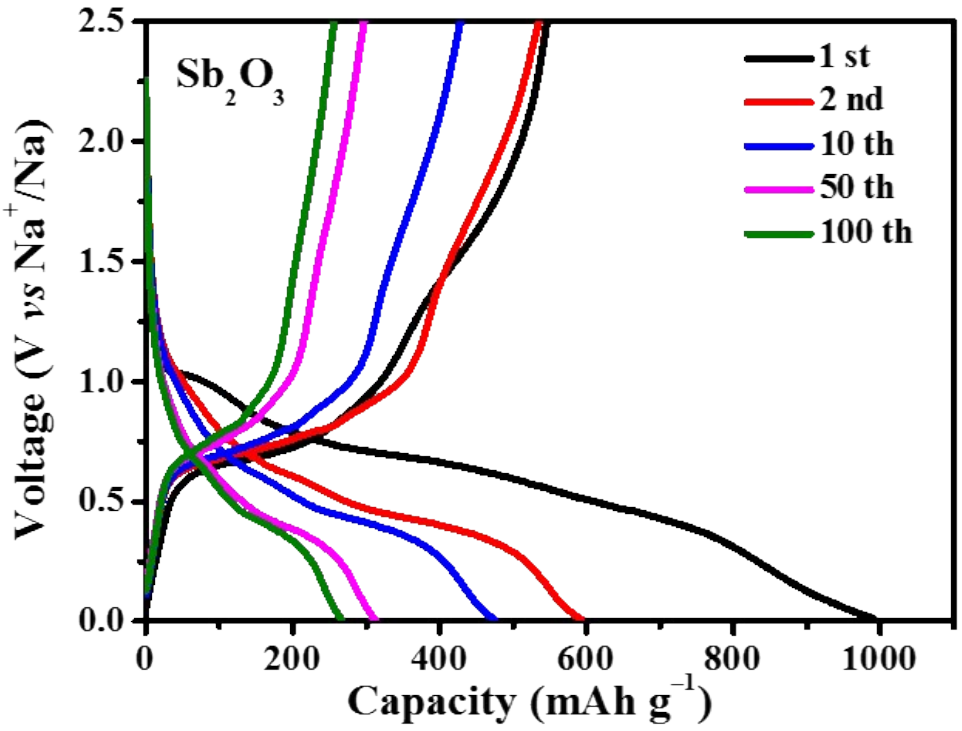

Fig S4. Charge/discharge curves of the bare Sb_2O_3 electrode at a current density of 0.1 Ag^{-1}.

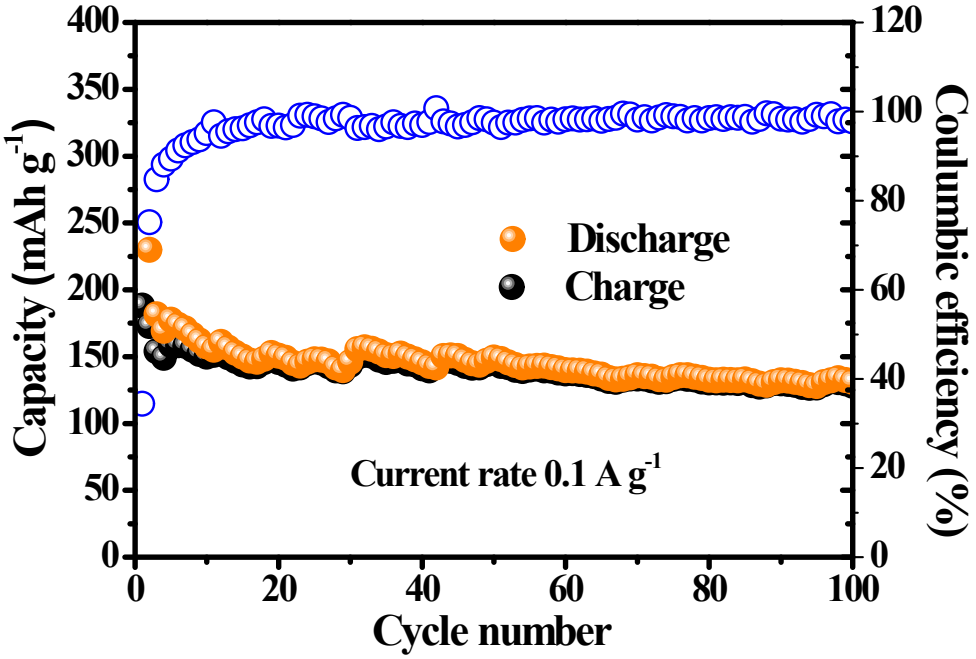

Fig S5. Cycling stability of RGO at the current density of 0.1 A g^{-1}.

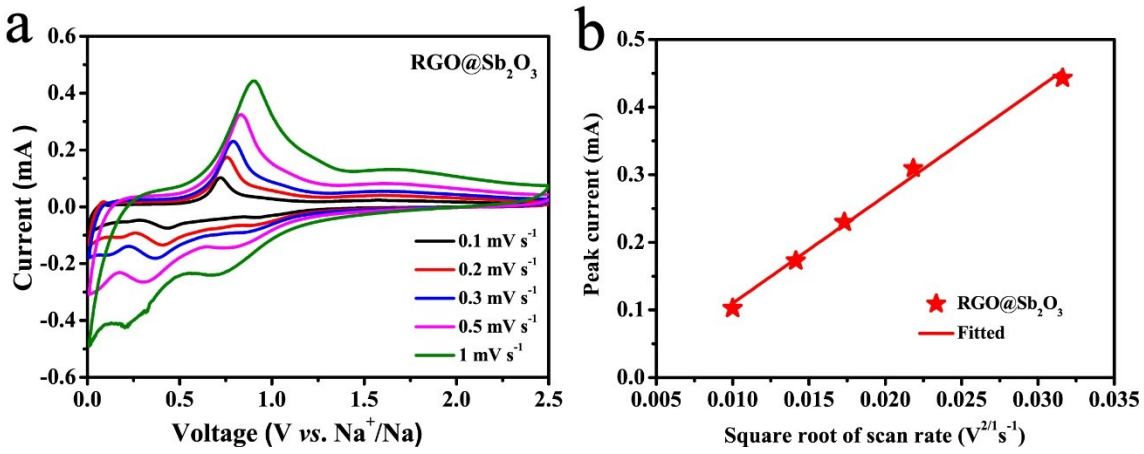

Fig S6. (a) CV curves of RGO@Sb_2O_3 electrode collected in the potential range of 0.01-2.5 V at scanning rates of 0.1, 0.2, 0.3, 0.5, and 1.0 mV s^{-1}. (b) The relationship between I_p and $v^{1/2}$ for RGO@Sb_2O_3 electrode.